Improvement of Tomo-PIV Analyses in the Nasal Cavities

Sandra Melina Tauwald[1,2,*], Florian Erzinger[2], Maurizio Quadrio[3], Markus Rütten[4], Christian Stemmer[5], and Lars Krenkel[1,2]
1: Regensburg Center of Health Sciences and Technology (RCHST), Germany
2: Dept. of Biofluidmechanics, Regensburg University of Applied Sciences (OTH), Germany
3: Dept. of Aerospace Science and Technology, Politechnico Milano, Italy
4: Institute of Aerodynamics and Flow Technology, German Aerospace Center (DLR), Germany
5: Chair of Aerodynamics and Fluid Mechanics, Technical University of Munich (TUM), Germany
* Correspondent author: melina.tauwald@oth-regensburg.de

Keywords: Tomo-PIV, Biomedical Flow, Non-Free-of-Sight, Breathing Cycle, Refractive Index Matching

The nasal cavities act as the main gateway to the entire respiratory system and thus play a pivotal role in respiratory homeostasis. The primary physiological function is for humidifying, warming, and particle filtering (Zubair et al., 2011). Indispensable for the physiological function is the sufficient contact of the respiratory air with the mucosa, the lining epithelium of the airways (Mlynski, 2013). Otorhinolaryngologists need detailed information of the flow regime in the patient-specific geometry in order to make a suitable diagnosis, preoperative planning, and thus achieve a successful surgery result. While the complex morphological structure of the nasal passageways is limited in access, the interaction of its anatomical form and its function requires investigations through either computational fluid dynamics (CFD) or in-vitro experiments (Doorly et al., 2008). The literature reveals investigations comprising CFD and/or experimental studies (Cozzi et al., 2017; Hörschler et al., 2006; Lintermann & Schröder, 2019). Nevertheless, the suitability of these investigations for the implementation to the medical field needs careful consideration. Emerging problems range from simplified geometries, neglecting the effects of cyclic respiratory flow, to the application of a suitable computational model (Zubair et al., 2011). These problems represent major challenges might be overcome by the hereinafter described tomo-PIV setup and investigations.

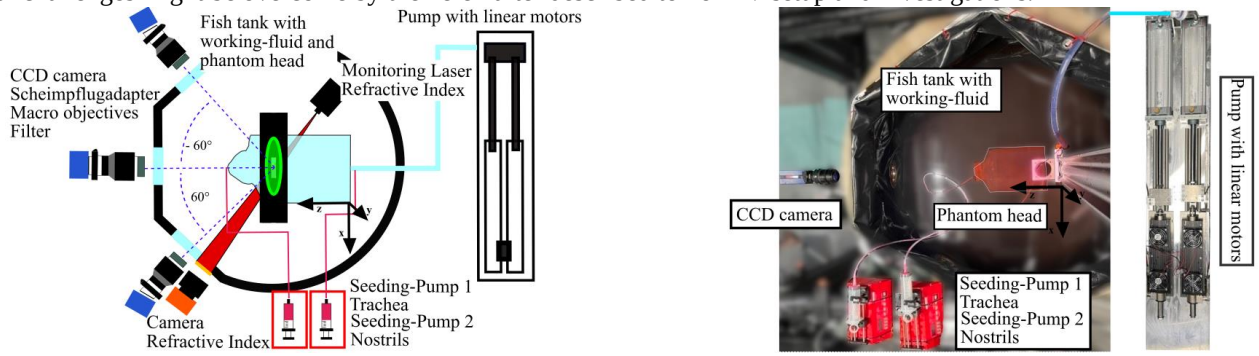

Figure 1. Experimental setup (sketch left, photograph right) in a top view including the RIM, the tomo-PIV setup and the flow inducing pump system.

The silicone model of the upper respiratory tract is based on a clinical computer tomographic (CT) scan (ethical approved) of a person's head. The experimental setup (figure 1) includes the model placed in a fish tank filled with working-fluid (WF) attached to a traversing unit. Three aspects have to be highlighted: the refractive index (RI) matching (RIM), the tomo-PIV setup, and the flow inducing part. The RIM monitoring contains a line laser placed vis-à-vis the 60° angled porthole. After passing the Region of Interest (RoI), the light sheet exiting the fish tank is visualized on a scaled paper and captured by a camera. Thereby, a kinked laser line on the scaled paper indicates a non sufficient matching of the RIs of the geometry and the WF. The tomo-PIV setup contains three CCD-cameras (1600x1200) equipped with macro objectives, Scheimpflug adapters, and cut-off filters. The tracer particles (20-50 µm) are induced by two syringe pumps, either via the trachea or via the nostrils, depending on the cycle state, and illuminated by a double-pulsed laser. The initial plate calibration of the cameras is refined for each RoI by a Volume Self Calibration (VSC). The volumetric reconstruction and vector calculation is fulfilled with a final window size of 40 voxels and a maximum expected displacement of 24 voxels. The RoIs are analyzed by several PIV-dts, depending on the cycle state and the geometry's shape. Whithin the flow inducing part, comprising a linear motor driven piston pump, the induced flow rate is based on test persons data adjusted by Reynolds and Womersley similarity, leading to a cycle period of 24.8 seconds, including the expiration part of 11.72 seconds. Thereby, peak flow rates are achieved at 6.0 seconds (0.370 l/s) for expiration and 17.7 seconds (-0.372 l/s) for inspiration. All components are centrally controlled by a

programmable logic controller. The in-place RIM monitoring showes the best results whithin a RI of 1.4139. The final achieved RoI reaches a size of 34 mm x 34 mm x 6 mm with a scale factor of 29 pix/mm.
Figure 2 shows velocity fields at three RoIs during inspiration at 15.9 seconds in the cycle, comprising a flow rate of -0.303 l/s and analyzed by a PIV-dt of 7 ms. The RoIs are located at the right nostril, ascending in direction of the conchae (boxes in figure 2 left). The exemplary xy-slices (I-III) show the coronal cross section perpendicular to the main direction of the flow (figure 2 upper part) and the yz-slices (I(z-axis)-III(z-axis)) show the saggittal section, indicated by the white dashed line. The colour coded magnitudes of velocities |V| reach up to 0.3 m/s. The gradients at the boundaries map the contours of the respective coronal cross-section in the geometry. The velocity profile shows a main flow in direction to the upper region of the main nasal cavities. However, this changes, visible at the yz-slices, the closer the RoI is to the conchae. Additionally, also in respect to the comparison of repeating cycles, unsteady peaks in the magnitude of velocity are visible.

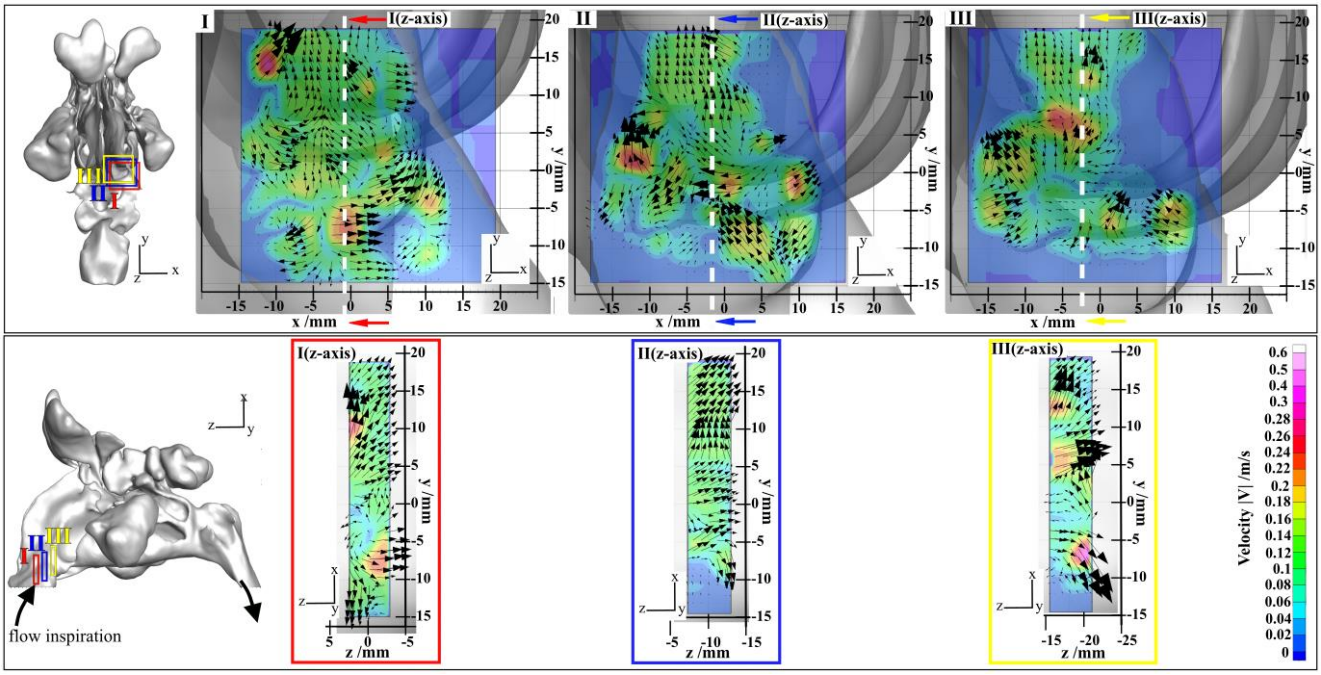

Figure 2. Examplary velocity profiles at three different RoIs. The left part indicates the positions in the geometry. The right part shows the magnitudes of velocity, colour coded, in a coronal section (upper part) and in a saggittal section (lower part).

While non-free-of-sight tomo-PIV investigations are sensitive to optical distortions, a preciese RIM is necessary to achieve a successfull calibration. The in-place RIM monitoring provides a precise RI control, leading to VSC-errors lower than 0.1 pixel. The defined seeding strategy of this study, adapted to the respective cycle phase enables a nearly homogenous tracer particle seeding and a sufficient seeding density. The marker particles in the geometry and a defined coordinate system of the geometry-moving traversing unit allows a matching of the small investigated RoIs into the micro CT-scan (STL-data, 11 mio faces) of the silicone head. This will give opportunities for an experimental validation of numerical investigations. Nevertheless, the highly complex geometry combined with a cyclic flow rate needs a detailed investigation of PIV-parameters, like PIV-dt and seeding strategies for each RoI. The experimental setup enables a high spatial resolution investigation and providing detailed information of the flow regime for several RoIs in the nasopharynx whithin different cycle states. The combination with the mico-CT scan of the geometry will provide a validation base for numerical investigations.

Cozzi, F., Felisati, G., & Quadrio, M. (2017). Velocity measurements in nasal cavities by means of stereoscopic PIV - preliminary tests. *J. Phys. Conf. Ser.* Advance online publication. https://doi.org/10.1088/1742-6596/882/1/012010

Doorly, D., Taylor, D. J., Franke, P., & Schroter, R. C. (2008). Experimental investigation of nasal airflow. *Proc Inst Mech Eng H*(222), 439–453. https://doi.org/10.1243/09544119JEIM330

Hörschler, I., Brücker, C., Schröder, W., & Meinke, M. (2006). Investigation of the impact of the geometry on the nose flow. *Eur. J. Mech.*(25), 471–490. https://doi.org/10.1016/j.euromechflu.2005.11.006

Lintermann, A., & Schröder, W. (2019). A Hierarchical Numerical Journey Trough the Nasal Cavity: From Nose-Like Models to Real Anatomies. *Flow Turbulence Combust.*(102), 89–116. https://doi.org/10.1007/s10494-017-9876-0

Mlynski, G. H. (Ed.). (2013). *Nasal Physiology and Pathophysiology of Nasal Disorders: Physiology and Pathophysiology of Nasal Breathing*. Springer. https://doi.org/10.1007/978-3-642-37250-6_20

Zubair, M., Abdullah, M. Z., Ismail, R., Shuaib, I. L., Hamid, S. A., & Ahmad, K. A. (2011). Review: A Critical Overview of Limitations of CFD Modeling in Nasal Airflow. *J Med Biol Eng.*(32), 77–84. https://doi.org/10.5405/jmbe.948